HHS Public Access

Author manuscript

Nat Commun. Author manuscript; available in PMC 2015 December 23.

Published in final edited form as:

Nat Commun. ; 6: 7466. doi:10.1038/ncomms8466.

A Metabolic Stress-inducible miR-34a-HNF4α Pathway Regulates Lipid and Lipoprotein Metabolism

Yang Xu[1], **Munaf Zalzala**[1], **Jiesi Xu**, **Yuanyuan Li**, **Liya Yin**, and **Yanqiao Zhang**

Department of Integrative Medical Sciences, Northeast Ohio Medical University, Rootstown, OH 44272, USA

Summary

Non-alcoholic fatty liver disease (NAFLD) is one of the most common liver diseases, but its underlying mechanism is poorly understood. Here we show that hepatocyte nuclear factor 4α (HNF4α), a liver-enriched nuclear hormone receptor, is markedly inhibited whereas miR-34a is highly induced in patients with non-alcoholic steatohepatitis, diabetic mice and mice fed a high fat diet. miR-34a is essential for HNF4α expression and regulates triglyceride accumulation in human and murine hepatocytes. miR-34a inhibits very low-density lipoprotein secretion and promotes liver steatosis and hypolipidemia in an HNF4α-dependent manner. As a result, increased miR-34a or reduced HNF4α expression in the liver attenuates the development of atherosclerosis in *Apoe*$^{-/-}$ or *Ldlr*$^{-/-}$ mice. These data indicate that the miR-34a-HNF4α pathway is activated under common conditions of metabolic stress and may have a role in the pathogenesis of NAFLD and in regulating plasma lipoprotein metabolism. Targeting this pathway may represent a novel approach for the treatment of NAFLD.

Introduction

Obesity, diabetes and insulin resistance are common risk factors for non-alcoholic fatty liver disease (NAFLD) [1–3], one of the most common liver diseases worldwide. In the US, up to 25% of the population have NAFLD [4,5]. NAFLD initiates from simple steatosis, which may progress to non-alcoholic steatohepatitis (NASH) after multiple “hits”, including inflammatory mediators, reactive oxygen species (ROS), etc [4,6,7]. NASH may further progress to liver cirrhosis and hepatocellular carcinoma. So far, the mechanism underlying the pathogenesis of NAFLD is poorly understood. Therefore, current treatment of NAFLD is limited to management of associated syndrome, such as diabetes and obesity [8,9].

Corresponding author: Yanqiao Zhang, MD, Department of Integrative Medical Sciences, Northeast Ohio Medical University, Phone: (330) 325-6693, Fax: (330) 325-5978, yzhang@neomed.edu.

[1]These authors contributed equally to this work

Author Contributions

Y. X. and M.Z. designed and performed the study and analyzed the data. J.X., Y.L., and L.Y. performed the study. Y.Z. designed and performed the study, analyzed the data and wrote the paper.

Competing Financial Interests

The authors declare no competing financial interests.

Hepatocyte nuclear factor 4α (HNF4α) is a nuclear hormone receptor that plays an important role in both development and adult physiology. It is highly expressed in the liver, with lower levels in the kidney, intestine and pancreatic β cells [10,11]. HNF4α has a highly conserved DNA binding domain and a ligand-binding domain. Structural analysis of HNF4α indicates that C14–C18 long-chain fatty acids are tightly bound to the hydrophobic pocket of HNF4α and could not be dissociated from the receptor under non-denaturing conditions [12,13]. As such, HNF4α is constitutively active.

HNF4α controls the basal expression of many genes involved in bile acid, lipid, glucose and drug metabolism. Loss-of-function mutations in human HNF4α cause maturity-onset diabetes of the young type 1 (MODY1), characterized by autosomal dominant inheritance, early-onset diabetes and pancreatic β-cell dysfunction [14]. The diabetes phenotype appears to result from reduced glucose-stimulated insulin secretion in the pancreas[15]. In addition to the diabetes phenotype, patients with MODY1 also have decreased plasma triglyceride (TG) and cholesterol levels[16–18], likely as a result of impaired very low-density lipoprotein (VLDL) secretion in the liver [19]. Consistent with the reduced VLDL secretion, we and others have shown that loss of hepatic HNF4α results in fatty liver and hypolipidemia in mice [19,20].

MicroRNAs (miRNAs) are small non-coding RNA molecules that regulate gene expression post-transcriptionally via binding to the 3′-untranslated region (3′UTR) of mRNA. miRNAs have emerged as important regulators of cell proliferation, inflammation and metabolism. Recent studies have shown that hepatic miRNAs may have an important impact on lipid and lipoprotein metabolism [21–23].

In this report, we investigate the role of the miR-34a-HNF4α pathway in the pathogenesis of human NAFLD and in plasma lipid and lipoprotein metabolism. Our data show that this pathway is activated in both NASH patients and diabetic or high fat diet (HFD)-fed mice. We then investigate whether and how this pathway regulates hepatic and plasma lipid and/or lipoprotein metabolism. Finally, we explore which metabolic cues triggere the activation of this pathway. Our data suggest that the miR-34a-HNF4α pathway may be an attractive target for treatment of human NAFLD.

Results

Inverse regulation of HNF4α and miR-34a expression in vivo

We and others have previously shown that loss of hepatic HNF4α causes fatty liver in mice [19,20]. Since HNF4α is highly conserved between humans and rodents, we explored the role of HNF4α in the development of human NAFLD. As compared to the normal subjects, NASH patients had increased levels of hepatic TG (Fig. 1a) and cholesterol (Fig. 1b). Remarkably, hepatic -*HNF4α* mRNA levels were reduced by 80% (Fig. 1c) and HNF4α protein levels were almost undetectable (Fig. 1d and Supplementary Fig. 1a) in NASH patients. Consistent with a marked reduction in hepatic HNF4α expression, a number of HNF4α target genes were also significantly reduced in NASH patients (Supplementary Table 1). miRNAs have been shown to play a role in the development of NAFLD [24,25]. In

the livers of NASH patients, *miR-34a* (Fig. 1e), but not *miR-19b* or *miR-27b* (Supplemental Fig. 1b), was induced by >2 fold.

NAFLD is often associated with obesity, diabetes and insulin resistance. Therefore, we investigated hepatic expression of HNF4α and miR-34a in diabetes and HFD-induced obesity. In *ob*/*ob* or *db*/*db* mice (type 2 diabetes models), streptozotocin (STZ)-treated mice (a type 1 diabetes model), HFD-fed mice or high fat/high cholesterol (HFHC) diet-fed mice, hepatic HNF4α protein levels were decreased by 75–85% (Fig. 1f–h **and** Supplementary Fig. 1c) whereas hepatic *miR-34a* levels were induced by up to 10 fold (Fig. 1i–l). In these mice, hepatic mRNA levels of *Hnf4α* (Supplementary Fig. 1d) or some *Hnf4α* target genes (Supplementary Table 2) were reduced or unchanged and hepatic *miR-19b* or *miR-27b* expression did not alter (Supplemental Fig. 1e). Finally, the data from Northern blot assays confirmed that hepatic *miR-34a* was over expressed in these models (Supplementary Fig. 2a–c). Together, these data indicate that hepatic HNF4α and miR-34a are inversely regulated in response to common metabolic stress.

miR-34a regulates HNF4α expression and lipid metabolism

To determine whether miR-34a regulates HNF4α expression and/or lipid metabolism, we injected adenoviruses expressing *miR-34a* (Ad-miR-34a) or Ad-empty (control) to C57BL/6 mice. Over-expression of *miR-34a* reduced plasma TG (Fig. 2a) and cholesterol (Fig. 2b) levels, increased hepatic TG levels by >2 fold (Fig. 2c) but had no effect on hepatic cholesterol levels (Supplementary Fig. 3). Over-expression of *miR-34a* also significantly reduced hepatic *Hnf4α* mRNA levels by 40% (Fig. 2d) and HNF4α protein levels by >75% (Fig. 2e, f). Consistent with the gain-of-function data, *miR-34a*$^{-/-}$ mice had increased plasma levels of TG (Fig. 2g) and cholesterol (Fig. 2h), decreased hepatic TG levels (Fig. 2i) and a 3.6-fold increase in hepatic HNF4α protein levels (Fig. 2j, k). A >3-fold increase in hepatic HNF4α protein levels was also observed in chow- or HFD-fed *miR-34a*$^{-/-}$ mice (Supplementary Fig. 4a–d). When *ob*/*ob* mice or HFD-fed mice were treated with an *miR-34a* antagomir, hepatic *miR-34a* levels were reduced by 84% and HNF4α protein levels were increased by >2 fold (Fig. 2l, m and Supplementary Fig. 5a–d). These gain- and loss-of-function data demonstrate that miR-34a regulates lipid metabolism and hepatic HNF4α expression in mice.

In HepG2 cells, a human hepatoma cell line, over-expression of miR-34a reduced HNF4α protein levels by 66% whereas inhibition of miR-34a expression by anti-miR-34a increased HNF4α expression by 2.2 fold (Fig. 2n, o). Consistent with a role of miR-34a in regulating lipid metabolism in mice, over-expression of miR-34a increased TG accumulation in HepG2 cells (Fig. 2p, q). Thus, the data of Fig. 2 demonstrate that miR-34a regulates HNF4α expression and lipid metabolism in both human and mouse hepatocytes.

miR-34a regulates lipid metabolism by inhibition of HNF4α

To determine how miR-34a regulates lipid metabolism, we analyzed hepatic gene expression. *miR-34a* inhibited a number of genes involved in lipid metabolism, including *Hnf4α*, microsomal triglyceride transfer protein (*Mtp*), *ApoB*, sterol regulatory element-binding protein 1c (*Srebp-1c*), acetyl-CoA carboxylase 1 (*Acc1*), *Acc2* and HMG-CoA

reductase (*Hmgcr*) (Fig. 3a). *miR-34a* also reduced MTP and ApoB protein levels (Fig. 3b, c **and** Supplementary Fig. 6a) and MTP activity (Supplementary Fig. 6b). In contrast, loss of *miR-34a* increased MTP activity (Supplementary Fig. 6c). Consistent with the latter data, *miR-34a* inhibited VLDL secretion (Fig. 3d). Interestingly, over-expression or loss of *miR-34a* had no effect on de novo lipogenesis (Supplementary Fig. 7).

A deficiency in hepatic HNF4α causes fatty liver and hypolipidemia by reducing VLDL secretion [20,21]. The data of Figs. 2 and 3a–d suggest that miR-34a regulates lipid metabolism likely through inhibition of HNF4α. To test this hypothesis, we over-expressed *Hnf4α* in mice infected with Ad-miR-34a in order to normalize hepatic HNF4α protein expression to the levels seen in the control mice (Fig. 3e). Hepatic over-expression of *miR-34a* reduced plasma levels of TG (Fig. 3f) and cholesterol (Fig. 3g) and increased hepatic TG levels (Fig. 3h) in the control mice. However, these changes were abolished when hepatic HNF4α protein expression was normalized (Fig. 3f–h). These data demonstrate that miR-34a regulates hepatic and plasma lipid metabolism through inhibition of hepatic HNF4α.

To understand how miR-34a regulates HNF4α expression, we investigated whether miR-34a binds to the *3′UTR* of *HNF4α*. There are two highly conserved miR-34a binding sites in both human and murine *3′UTRs* of *HNF4α* (Supplemental Fig. 8a, b). As shown in Fig. 3i, an miR-34a mimic significantly repressed the activity of a luciferase promoter linked to the *Hnf4α 3′UTR* and this repression was abolished when the second binding site for *miR-34a* (mutB) was mutated. To confirm the *in vitro* data, we over-expressed *Hnf4α* coding region plus wild-type or mutant *3′UTR* in liver-specific *Hnf4α*$^{-/-}$ mice. Over-expression of *miR-34a* markedly reduced exogenous HNF4α protein levels when the *Hnf4α* coding region was linked to the wild-type *3′UTR* or *3′UTR* with mutations in first binding site for miR-34a (mutA), and this reduction was abolished when the *Hnf4α* coding region was linked to *3′UTR* with mutB (Fig. 3j). Thus, our *in vitro* and *in vivo* data demonstrate that *miR-34a* inhibits *Hnf4α* expression through binding to the second binding site of the *3′UTR*.

Hepatic HNF4α regulates atherogenesis and energy metabolism

Loss-of-function mutations in HNF4α cause hypolipidemia in MODY patients. So far, it is unknown whether MODY1 patients are protective against the development of atherosclerosis. Given that hepatic HNF4α is markedly down-regulated under various metabolic stress (Fig. 1), we investigated the effect of acute vs. chronic loss of hepatic HNF4α on the development of atherosclerosis. Acute knockdown of hepatic *Hnf4α* by shRNA in *Apoe*$^{-/-}$ mice for three weeks caused a >50% reduction in plasma total cholesterol levels and a ~ 30% reduction in plasma TG on a Western diet (Supplementary Fig. 9a–c). Analysis of plasma lipoprotein profiles by fast protein liquid chromatography (FPLC) indicated that loss of hepatic *Hnf4α* reduced plasma VLDL cholesterol and LDL cholesterol (Fig. 4a) and VLDL TG (Fig. 4b). Consistent with the changes in plasma lipids and lipoproteins, acute knockdown of hepatic *Hnf4α* in *Apoe*$^{-/-}$ mice reduced aortic lesion sizes by >50% (Fig. 4c **and** Supplementary Fig. 9d). In addition, loss of hepatic *Hnf4α* in *Apoe*$^{-/-}$ mice increased hepatic TG accumulation (Fig. 4d) and reduced MTP and ApoB protein expression (Supplementary Fig. 9e). These data indicate that acute loss of hepatic HNF4α reduces the development of atherosclerosis in *Apoe*$^{-/-}$ mice.

To determine whether chronic loss of hepatic HNF4α has a similar effect on atherosclerosis, we crossed *HNF4α*$^{fl/fl}$ mice with *Ldlr*$^{-/-}$ mice. These mice were then crossed with albumin-Cre mice to generate double knockout (DKO) mice deficient in both *Ldlr* and hepatic *Hnf4α* as well as control (*Ldlr*$^{-/-}$*HNF4α*$^{fl/fl}$) mice. As compared to the control mice, the DKO mice had increased food intake (Supplementary Fig. 10a) but gained less body weight (Fig. 4e) and body fat content (Fig. 4f), and had increased O_2 consumption and CO_2 production (Fig. 4g–i) as well as heat production (Fig. 4j). Mechanistically, DKO mice had increased *Cpt1b* expression in the liver (Supplementary Fig. 10b, c), suggesting that hepatic fatty acid oxidation may be increased in these mice. In addition, the DKO mice had a >50% reduction in plasma cholesterol (Fig. 4k) and TG (Fig. 4L), and these changes were due to a marked reduction in plasma VLDL cholesterol and LDL cholesterol (Fig. 4M) and VLDL TG (Fig. 4N), respectively. ln agreement with the change in plasma lipid profile, DKO mice had a >50% reduction in the lesion size of aortic root (Fig. 4o, p), brachiocephalic artery (Fig. 4q) or aorta (Fig. 4r, s). Finally, consistent with a role of hepatic HNF4α in controlling VLDL secretion, DKO mice had reduced VLDL secretion (Fig. 4t). Thus, chronic loss of hepatic *Hnf4α* in *Ldlr*$^{-/-}$ mice increases energy expenditure and protects against the development of atherosclerosis.

Hepatic *miR-34a* inhibits atherogenesis in *Ldlr*$^{-/-}$ mice

The finding that miR-34a regulates lipid metabolism through inhibition of HNF4α (Fig. 3) led us to ask whether miR-34a also regulates the development of atherosclerosis. Over-expression of *miR-34a* in Western diet-fed *Ldlr*$^{-/-}$ mice reduced plasma total cholesterol (Fig. 5a) and TG levels (Fig. 5b). The data from FPLC analysis showed that *miR-34a* reduced the levels of VLDL and LDL cholesterol (Fig. 5c) as well as VLDL TG (Fig. 5d). As a result, over-expression of *miR-34a* in the liver reduced the atherosclerotic lesion size by >50% in both the aortic root (Fig. 5e, 5f) and aorta (Fig. 5g, h) of *Ldlr*$^{-/-}$ mice. In the liver, over-expression of *miR-34a* in *Ldlr*$^{-/-}$ mice inhibited hepatic HNF4α, ApoB100 and ApoB48 expression (Fig. 5i) and increased hepatic TG levels (Supplementary Fig. 11). Thus, either over-expression of hepatic miR-34a (Fig. 5) or inhibition of hepatic HNF4α (Fig. 4) can provide protection against the development of atherosclerosis.

p53, FFAs and cholesterol regulate the miR-34a-HNF4α pathway

The finding that the miR-34a-HNF4α pathway is highly induced under common metabolic stress and regulates lipid and lipoprotein metabolism is quite intriguing. However, it remains to be determined which metabolic cue(s) trigger this pathway. p53 is an oxidative stress-inducible protein and is shown to both up-regulate miR-34a expression [26–29] and promote liver steatosis [30,31]. Indeed, nuclear p53 protein levels were induced by 6.7 fold in NASH patients (Fig. 6a, b). Interestingly, p53 protein levels were unchanged in diabetic mice or HFD-induced mice (Supplemental Fig. 12a–c). Over-expression of p53 in HepG2 cells significantly induced *miR-34a* expression (Supplementary Fig. 13) and reduced HNF4α protein level (Fig. 6c). The data of Fig. 6a–c, together with previous observations [26–31], suggest that p53 may contribute to the induction of the miR-34a-HNF4α pathway and liver steatosis in NASH patients.

Obesity, diabetes and insulin resistance are common risk factors for NAFLD, which is associated with higher levels of free fatty acids (FFAs), cholesterol, insulin and/or glucose in the blood and/or tissues. Treatment of HepG2 cells with palmitate (Fig. 6d), linoleic acid (Fig. 6e), oleic acid (Fig. 6f) or cholesterol (Fig. 6g) significantly reduced HNF4α expression (Fig. 6d–h). In contrast, insulin or glucose treatment had no effect on HNF4α expression in HepG2 cells (Supplementary Fig. 14a, b). Treatment with palmitate, linoleic acid or oleic acid also significantly increased *miR-34a* expression in HepG2 cells (Fig. 6I). Similar results were also observed when the murine primary hepatocytes were used (Supplementary Fig. 14c–e). Together, our data suggest that FFAs, cholesterol and p53 are upstream activators for the miR-34a-HNF4α pathway in diabetes, obesity and NASH (Fig. 6J)

Discussion

NAFLD is one of the most common liver diseases worldwide. However, the underlying mechanism remains elusive. Here we report that a novel miR-34a-HNF4α pathway regulates both hepatic TG levels and plasma lipid and lipoprotein metabolism. Given that this pathway is activated under common metabolic stress (diabetes, HFD feeding and NASH), this pathway may represent a common mechanism leading to the pathogenesis of human NAFLD. Targeting the miR-34a-HNF4α pathway may be an attractive approach to treatment of NAFLD.

The finding that hepatic HNF4α is markedly reduced in diabetes, obesity and NASH is quite intriguing. In NASH patients, hepatic HNF4α protein is almost absent. Consistent with this finding, the vast majority of HNF4α target genes, including those involved in bile acid metabolism, blood coagulation, lipid and lipoprotein metabolism, xenobiotic/drug metabolism and liver differentiation (HNF1α), are significantly reduced in NASH patients (Supplementary table 1). Previous data show that HNF4α also regulate genes involved in urea synthesis in mice [32]. We do not see any change in genes involved in urea synthesis in NASH patients, which could be due to the difference in species. In HFD-fed mice, hepatic HNF4α protein is reduced only by ~ 80%. As a result, some of the known *Hnf4α* target genes are also reduced whereas some others remain unchanged in these mice (Supplementary table 2). Other yet-to-be-determined factors may also contribute to the selective regulation of HNF4α target genes in the HFD-fed mice.

Previous studies have shown that *miR-34a* is induced in NAFLD patients [33,34] and obese/diabetic mice [35,36]. However, whether or how miR-34a regulates hepatic TG metabolism has not been addressed previously. Here we show that increased *miR-34a* expression results in TG accumulation whereas inhibition or ablation of *miR-34a* expression reduces TG accumulation in both mice and HepG2 cells. By using human NASH patient samples and various diabetes and obesity mouse models, we conclude that miR-34a and HNF4α are inversely regulated under all the common metabolic stress. Recently, Lamba *et al.* also observed a negative correlation between hepatic miR-34a and HNF4α expression in humans [37], further supporting our finding. The finding that miR-34a inhibits HNF4α expression has led us to hypothesize that miR-34a regulates hepatic TG levels via inhibition of HNF4α. Such a hypothesis is validated by our subsequent studies. Our previous studies

demonstrate that loss of hepatic HNF4α has no effect on hepatic TG biosynthesis but causes liver steatosis by reducing VLDL secretion [19]. Consistent with our previous finding, miR-34a reduces VLDL secretion and has no effect on de novo lipogenesis (Supplementary Fig. 7). Thus, our current work not only reveals a novel function for miR-34a in regulating hepatic TG metabolism, but also elucidates how miR-34a regulates hepatic TG metabolism.

Choi *et al*. reported that miR-34a also reduces NAD^+ levels and SIRT1 activity by targeting NAMPT [38], the rate-limiting enzyme of NAD^+ synthesis. Although SIRT1 is known to play an important role in metabolic control, including hepatic TG metabolism, it remains to be determined whether SIRT1 plays a role in miR-34a-regulated TG metabolism. According to our compelling data, miR-34a increases hepatic TG levels by inhibition of HNF4α. Interestingly, over-expression of miR-34a selectively regulates some of the HNF4α target genes (Fig. 3), which could result from incomplete inhibition of HNF4α expression and HNF4α-independent gene regulation.

Another important finding of this study is that we demonstrate that the miR-34a-HNF4α pathway also regulates plasma ApoB-containing lipoprotein metabolism and the development of atherosclerosis. Increased plasma levels of ApoB-containing lipoproteins are known to accelerate the development of atherosclerosis. Our data show that the miR-34a-HNF4α pathway promotes hypolipidemia by inhibition of VLDL secretion. In line with this finding, it has been reported that NASH patients have reduced VLDL secretion [39]. As a result of the hypolipidemia, either over-expression of *miR-34a* or inhibition/ablation of hepatic *Hnf4α* expression prevents the development of atherosclerosis in $Apoe^{-/-}$ mice or $Ldlr^{-/-}$ mice. These data provides the first evidence demonstrating that the miR-34a-HNF4α pathway regulates the development of atherosclerosis. Based on our studies, it will be interesting to investigate whether NASH patients and/or MODY1 patients are protective against atherosclerosis.

In addition to elucidating the role of the miR-34a-HNF4α pathway in regulating lipid and lipoprotein metabolism, we also investigated how this pathway is activated under common metabolic stress. Our data suggest that the miR-34a-HNF4α pathway is activated in both p53-dependent and p53-independent manners (Fig. 6j). In NASH patients, p53, FFAs and cholesterol may work together to activate the miR-34a-HNF4α pathway. However, p53 is not activated in diabetes or HFD-induced obesity. Thus, under these latter conditions, FFAs and cholesterol may be the major factors triggering activation of the miR-34a-HNF4α pathway. One of our future directions will be to investigate how FFAs and cholesterol activate the miR-34a-HNF4α pathway and whether other metabolic cues are also involved in regulation of this pathway.

In summary, the current study has demonstrated that the metabolic stress-inducible miR-34a-HNF4α pathway may play a critical role in both the pathogenesis of NAFLD and regulating plasma lipid and lipoprotein metabolism. Although loss of hepatic HNF4α has a beneficial effect on atherosclerosis and energy homeostasis, loss of hepatic HNF4α causes fatty liver by inhibiting VLDL secretion. Thus, from therapeutic standpoint, suppression of hepatic HNF4α expression together with approaches that alleviate hepatic steatosis may be useful for preventing the development of atherosclerosis. In contrast, over-expression of

hepatic HNF4α does not have much effect on plasma lipid or lipoprotein metabolism likely because HNF4α is one of the most abundant genes in the liver [19]. Given that HNF4α expression is markedly reduced under metabolic stress (diabetes, HFD feeding and NASH), delivery of HNF4α via adeno-associated virus or other gene therapy vehicle(s) is a feasible and attractive approach to prevention and treatment of NAFLD associated with metabolic syndrome. In addition, antagonism of hepatic miR-34a function by antagomir(s) is also a feasible approach that may help prevent the development of NAFLD. Thus, targeting the miR-34a-HNF4α pathway represents a promising and attractive approach for treatment of human NAFLD.

Methods

Human liver tissues, mice and diets

C57BL/6, *ob*/*ob*, *db*/*db*, *Hnf4α*$^{fl/fl}$, *Ldlr*$^{-/-}$, *miR-34a*$^{-/-}$ mice and albumin-Cre (Alb-Cre) mice were purchased from the Jackson Laboratories (Bar Harbor, Maine). *Hnf4α*$^{fl/fl}$ mice were crossed with *Ldlr*$^{-/-}$ mice to produce *Hnf4α*$^{fl/fl}$*Ldlr*$^{-/-}$ mice, which were subsequently crossed with Alb-Cre mice to produce liver-specific *Hnf4α*$^{-/-}$*Ldlr*$^{-/-}$ (*L-Hnf4α*$^{-/-}$*Ldlr*$^{-/-}$) mice. For streptozotocin (STZ) treatment, C57BL/6J mice were injected intraperitoneally (i.p.) with either vehicle (0.1M sodium citrate, pH 4.5) or STZ (50 mg/kg) for 5 days and then euthanized 5 weeks after the treatment. For high fat diet (HFD) feeding, C57BL/6J mice were fed a chow diet or an HF diet (60% kcal from fat; Research Diets, New Brunswick, NJ, USA) for 16 weeks. For high fat, high cholesterol (HFHC) diet feeding, C57BL/6J mice were fed a chow diet or an HFHC diet (42% kcal fat/0.2% cholesterol; Harlan Teklad, Madison, Wisconsin, USA) for 3 weeks. Unless otherwise stated, male and age-matched (8–12 weeks old) mice were randomly assigned to groups and all mice were fasted for 5–6 h prior to euthanization. Mice that did not look healthy were excluded in the studies. Human liver samples were obtained from the Liver Tissue Cell Distribution System at University of Minnesota. Both male and female individuals were included. The average ages for normal individuals and NASH patients were 55.8 and 52.5 year old, respectively. Individuals with alcohol drinking history (2–3 drinks/day) and liver cancer were excluded from the study. All the animal experiments were approved by the Institutional Animal Care and Use Committee at Northeast Ohio Medical University (NEOMED) and the use of human tissue samples were approved by the Institutional Review Board at NEOMED.

Mutagenesis, transfections and cell culture

HepG2 cells were purchased from ATCC (Virginia) and cultured in DMEM plus 10% FBS. *3′-UTR* of mouse *Hnf4α* was cloned to the Mlu/PmeI sites of pMIR-Report (catalog AM5795, Life Technologies). Potential miR-34a binding site A (232–238 nt) and site B (2710–2716 nt) were mutated using a mutagenesis kit from Agilent (catalog 210518). The forward primer sequences for the mutant binding site A (mutA) and the mutant binding site B (mutB) are 5′-gagaagaccccagggaggactgtcttc**ggtctag**tggactcctctcaagttgaagtcatcgtc-3′ and cctaccctgat ccccaaggccccaccat**ggtctag**caaggggtaaaaaagagaaaaagccctc, respectively (mutations are indicated in bold). An miR-34a mimic (C-310529-07-0005) and a control mimic were purchased from Dhmarcon (Thermo Scientific). Transfections were performed using Lipofectamin 2000 (catalog 11668019, Life Technologies). The miRNA mimics were

transfected at a final concentration of 50 nM. For treatment with FAs or cholesterol, HepG2 cells or primary hepatocytes were cultured in serum-free DMEM, then treated with either vehicle or palmitate (300 μM), oleic acid (300 μM), linoleic acid (300 μM) or cholesterol (10 μg/ml). Cells were harvested 48–72 hours later for luciferase or Western blot assays or lipid extraction.

Adenoviruses

Ad-shLacZ, Ad-HNF4α, Ad-shHNF4α, Ad-empty (control) and Ad-miR-34a have been described previously [19,35]. When Ad-HNF4α was constructed, only the *Hnf4α* coding region (which does not include any 3′UTR) was cloned into the adenoviral vector. In contrast, Ad-HNF4α-3′UTR, Ad-HNF4α-3′UTR_mutA and Ad-HNF4α-3′UTR_mutB were generated by cloning the *Hnf4α* coding region plus wild-type or mutant *3′UTR* (with mutA or mutB) into a pAd/CMV/V5-Dest vector (catalog V493-20, Life Technologies), followed by transfection into 293 cells for adenovirus production [40]. Ad-p53 was purchased from Vector Biolabs (cat # 1168). Ad-anti-miR-34a was generated by Applied Biological Materials (British Columbia, Canada). Cells were infected with adenoviruses at an MOI of 5. Mice were intravenously (i.v.) injected with 0.5–1.5 $\times 10^9$ pfu adenoviruses. Unless otherwise stated, the mice were euthanized 7 days post infection.

Real-time PCR

RNA was isolated using TRIzol Reagent (Life Technologies, CA). miRNAs were isolated using mirVana™ miRNA isolation kit (Life Technologies, cA). mRNA levels were determined by quantitative reverse-transcription polymerase chain reaction (qRT-PCR) on a 7500 real-time PCR machine from Applied Biosystems (Foster City, CA) by using SYBR Green Supermix (Roche, Indianapolis, IN). Results were calculated using *Ct* values and normalized to *36B4* mRNA level. miRNA levels were quantified using TaqMan primers and probes (Catalog 4427975, Life Technologies, CA) and normalized to U6 levels.

MicroRNA Northern blot assays

microRNA levels were also determined by Northern blot assays following the manufacturer's instructions (Signosis, Santa Clara, CA. Cat # NB-1001). In the Northern blot assays, robes for miR-34a (Catalog MP-0602) and U6 (Catalog MP-0512) were also from Signosis.

MTP activity assays

Liver was homogenized and MTP activity was measured following the manufacturer's instructions (Chylos, Inc, Woodbury, NY. Cat #R100).

Western blot assays

Western blot assays were performed using whole liver lysates [41] or nuclear proteins of the liver samples and images were collected by ImageQuant LAS 4000 (GE Healthcare, Pittsburgh, PA) [42]. MTP antibody (catalog sc-135994), HNF4α antibody (catalog sc-6556) and p53 antibody (catalog sc-6243) were purchased from Santa Cruz Biotechnology (Santa Cruz, CA). ApoB antibody was purchased from Meridian Life Science (K45253G, TN). β-

actin antibody was from Novus Biologicals (catalog NB600-501, CO). Histone antibody was from Cell Signaling (Beverly, MA). The antibodies were used at a concentration of 1 μg per ml.

Antagomirs

miR-34a LNA inhibitor/antagomir (LNA-miR-34a; anta-miR-34a; anta-34a) and miRNA scramble LNA inhibitor/antagomir (LNA-scr; anta-scr) were synthesized by Exiqon (Denmark, Cat # 199900). *ob*/*ob* mice or HFD-fed mice (fed an HF diet for 12 weeks) were injected i.v. with either anta-miR-34a or anta-scr once every 6 days (10 mg per kg). After 3 injections, mice were euthanized.

Lipid and lipoprotein analysis

Approximately 100 mg liver was homogenized in methanol and lipids were extracted in chloroform/methanol (2:1 v/v) as described [43]. Hepatic triglyceride and cholesterol levels were then quantified using Infinity reagents from Thermo Scientific (Waltham, MA). Plasma lipid and glucose levels were also determined using Infinity reagents. Plasma lipoprotein profile was analyzed by FPLC as described [19]. Briefly, after 100 μl plasma was injected, lipoproteins were run at 0.5 ml/min in a buffer containing 0.15 M NaCl, 0.01 M Na_2HPO4, 0.1 mM EDTA, pH 7.5, and separated on a Superose 6 10/300 GL column (GE Healthcare) by using BioLogic DuoFlow QuadTec 10 System (Bio-Rad, CA). 500 μl of sample per fraction was collected.

VLDL secretion

C57BL/6J mice were injected intravenously with specific adenoviruses. On day 6, these mice were fasted overnight, followed by intravenous injection of Tyloxapol (500 mg/kg). Blood was taken at indicated time points and plasma TG levels determined.

De novo lipogenesis

Mice were injected i.p. with heavy water (^2H2O) to reach 3% enrichment. After 4 hours, livers were collected. Labeled and unlabeled palmitate, glycerol (triglycerides) and cholesterol were analyzed by mass spectrometry [19,44].

Atherosclerotic lesions

The aorta and aortic root were isolated and dissected. The aortic root was washed with phosphate-buffered saline, embedded in optimal cutting temperature compound, and then frozen on dry ice. Serial 7-μm-thick cryosections from the middle portion of the ventricle to the aortic arch were collected on superfrost plus microscope slides (Catalog 12-550-15, Fisher Scientific). In the region beginning at the aortic valves, every other section was collected. Sectioned aortic root or *en face* aorta was stained with oil red O and the atherosclerotic lesion size determined using Image-Pro Premier 9.0 (Media Cybernetics, Rockville, MD) [45].

Energy expenditure

Mice fed a Western diet were put in the Comprehensive Lab Animal Monitoring System (CLAMS). Oxygen consumption, CO_2 production and heat production were determined [46]. Briefly, Mice were put in the acclimation cages for 40–48 h. After the acclimation period, mice were weighed and placed back into the acclimation cage with pre-weighed food. Gas exchange was measured in mice every 30 seconds. Room air was pumped into the mouse calorimetry cages at 0.472–0.600 liters per minute (LPM) and cage air was sampled at 0.4 LPM. Physical activity was measured simultaneously using 16 infrared sensors spread over 19 cm. Data from noon on day 1 to noon on day 2 (EST) were selected for analysis.

Statistical analysis

Statistical significance was analyzed using unpaired two-sided Student *t* test or ANOVA (GraphPad Prisim, CA). All values are expressed as mean±SEM. Differences were considered statistically significant at $P<0.05$.

Supplementary Material

Refer to Web version on PubMed Central for supplementary material.

Acknowledgments

This work was supported by NIH grants R15DK088733, R01HL103227, R01DK095895 and R01DK102619 to Y.Z. Normal or pathologic human liver tissues were obtained through the Liver Tissue Cell Distribution System, Minneapolis, Minnesota, which was funded by NIH Contract # HHSN276201200017C.

References

1. Petersen KF, et al. Reversal of nonalcoholic hepatic steatosis, hepatic insulin resistance, and hyperglycemia by moderate weight reduction in patients with type 2 diabetes. Diabetes. 2005; 54:603–608. [PubMed: 15734833]
2. Yki-Jarvinen H. Fat in the liver and insulin resistance. Ann Med. 2005; 37:347–356. [PubMed: 16179270]
3. Anstee QM, Goldin RD. Mouse models in non-alcoholic fatty liver disease and steatohepatitis research. Int J Exp Pathol. 2006; 87:1–16. [PubMed: 16436109]
4. Angulo P. Nonalcoholic fatty liver disease. N Engl J Med. 2002; 346:1221–1231. [PubMed: 11961152]
5. Li Y, Jadhav K, Zhang Y. Bile acid receptors in non-alcoholic fatty liver disease. Biochem Pharmacol. 2013; 86:1517–1524. [PubMed: 23988487]
6. Day CP, James OF. Steatohepatitis: a tale of two “hits”? Gastroenterology. 1998; 114:842–845. [PubMed: 9547102]
7. Farrell GC, Larter CZ. Nonalcoholic fatty liver disease: from steatosis to cirrhosis. Hepatology. 2006; 43:S99–S112. [PubMed: 16447287]
8. Angulo P. Treatment of nonalcoholic fatty liver disease. Ann Hepatol. 2002; 1:12–19. [PubMed: 15114291]
9. Lewis JR, Mohanty SR. Nonalcoholic fatty liver disease: a review and update. Dig Dis Sci. 2010; 55:560–578. [PubMed: 20101463]
10. Drewes T, Senkel S, Holewa B, Ryffel GU. Human hepatocyte nuclear factor 4 isoforms are encoded by distinct and differentially expressed genes. Mol Cell Biol. 1996; 16:925–931. [PubMed: 8622695]

11. Jiang S, et al. Expression and localization of P1 promoter-driven hepatocyte nuclear factor-4alpha (HNF4alpha) isoforms in human and rats. Nucl Recept. 2003; 1:5. [PubMed: 12952540]
12. Dhe-Paganon S, Duda K, Iwamoto M, Chi YI, Shoelson SE. Crystal structure of the HNF4 alpha ligand binding domain in complex with endogenous fatty acid ligand. J Biol Chem. 2002; 277:37973–37976. [PubMed: 12193589]
13. Wisely GB, et al. Hepatocyte nuclear factor 4 is a transcription factor that constitutively binds fatty acids. Structure. 2002; 10:1225–1234. [PubMed: 12220494]
14. Fajans SS, Bell GI, Polonsky KS. Molecular mechanisms and clinical pathophysiology of maturity-onset diabetes of the young. N Engl J Med. 2001; 345:971–980. [PubMed: 11575290]
15. Miura A, et al. Hepatocyte nuclear factor-4alpha is essential for glucose-stimulated insulin secretion by pancreatic beta-cells. J Biol Chem. 2006; 281:5246–5257. [PubMed: 16377800]
16. Lehto M, et al. Mutation in the HNF-4alpha gene affects insulin secretion and triglyceride metabolism. Diabetes. 1999; 48:423–425. [PubMed: 10334325]
17. Shih DQ, et al. Genotype/phenotype relationships in HNF-4alpha/MODY1: haploinsufficiency is associated with reduced apolipoprotein (AII), apolipoprotein (CIII), lipoprotein(a), and triglyceride levels. Diabetes. 2000; 49:832–837. [PubMed: 10905494]
18. Pramfalk C, et al. Control of ACAT2 liver expression by HNF4{alpha}: lesson from MODY1 patients. Arterioscler Thromb Vasc Biol. 2009; 29:1235–1241. [PubMed: 19478207]
19. Yin L, Ma H, Ge X, Edwards PA, Zhang Y. Hepatic hepatocyte nuclear factor 4alpha is essential for maintaining triglyceride and cholesterol homeostasis. Arterioscler Thromb Vasc Biol. 2011; 31:328–336. [PubMed: 21071704]
20. Hayhurst GP, Lee YH, Lambert G, Ward JM, Gonzalez FJ. Hepatocyte nuclear factor 4alpha (nuclear receptor 2A1) is essential for maintenance of hepatic gene expression and lipid homeostasis. Mol Cell Biol. 2001; 21:1393–1403. [PubMed: 11158324]
21. Fernandez-Hernando C, Suarez Y, Rayner KJ, Moore KJ. MicroRNAs in lipid metabolism. Current opinion in lipidology. 2011; 22:86–92. [PubMed: 21178770]
22. Sacco J, Adeli K. MicroRNAs: emerging roles in lipid and lipoprotein metabolism. Current opinion in lipidology. 2012; 23:220–225. [PubMed: 22488426]
23. Soh J, Iqbal J, Queiroz J, Fernandez-Hernando C, Hussain MM. MicroRNA-30c reduces hyperlipidemia and atherosclerosis in mice by decreasing lipid synthesis and lipoprotein secretion. Nature medicine. 2013; 19:892–900.
24. Cheung O, Sanyal AJ. Role of microRNAs in non-alcoholic steatohepatitis. Current pharmaceutical design. 2010; 16:1952–1957. [PubMed: 20370674]
25. Rottiers V, Naar AM. MicroRNAs in metabolism and metabolic disorders. Nature reviews Molecular cell biology. 2012; 13:239–250. [PubMed: 22436747]
26. Raver-Shapira N, et al. Transcriptional activation of miR-34a contributes to p53-mediated apoptosis. Molecular cell. 2007; 26:731–743. [PubMed: 17540598]
27. Chang TC, et al. Transactivation of miR-34a by p53 broadly influences gene expression and promotes apoptosis. Molecular cell. 2007; 26:745–752. [PubMed: 17540599]
28. Tarasov V, et al. Differential regulation of microRNAs by p53 revealed by massively parallel sequencing: miR-34a is a p53 target that induces apoptosis and G1-arrest. Cell cycle. 2007; 6:1586–1593. [PubMed: 17554199]
29. He L, et al. A microRNA component of the p53 tumour suppressor network. Nature. 2007; 447:1130–1134. [PubMed: 17554337]
30. Derdak Z, et al. Inhibition of p53 attenuates steatosis and liver injury in a mouse model of non-alcoholic fatty liver disease. J Hepatol. 2013; 58:785–791. [PubMed: 23211317]
31. Yahagi N, et al. p53 involvement in the pathogenesis of fatty liver disease. J Biol Chem. 2004; 279:20571–20575. [PubMed: 14985341]
32. Inoue Y, Hayhurst GP, Inoue J, Mori M, Gonzalez FJ. Defective ureagenesis in mice carrying a liver-specific disruption of hepatocyte nuclear factor 4alpha (HNF4alpha). HNF4alpha regulates ornithine transcarbamylase in vivo. J Biol Chem. 2002; 277:25257–25265. [PubMed: 11994307]
33. Cheung O, et al. Nonalcoholic steatohepatitis is associated with altered hepatic MicroRNA expression. Hepatology. 2008; 48:1810–1820. [PubMed: 19030170]

34. Cermelli S, Ruggieri A, Marrero JA, Ioannou GN, Beretta L. Circulating microRNAs in patients with chronic hepatitis C and non-alcoholic fatty liver disease. PloS one. 2011; 6:e23937. [PubMed: 21886843]
35. Lee J, et al. A pathway involving farnesoid X receptor and small heterodimer partner positively regulates hepatic sirtuin 1 levels via microRNA-34a inhibition. J Biol Chem. 2010; 285:12604–12611. [PubMed: 20185821]
36. Trajkovski M, et al. MicroRNAs 103 and 107 regulate insulin sensitivity. Nature. 2011; 474:649–653. [PubMed: 21654750]
37. Lamba V, Ghodke Y, Guan W, Tracy TS. microRNA-34a is associated with expression of key hepatic transcription factors and cytochromes P450. Biochemical and biophysical research communications. 2014; 445:404–411. [PubMed: 24530915]
38. Choi SE, et al. Elevated microRNA-34a in obesity reduces NAD+ levels and SIRT1 activity by directly targeting NAMPT. Aging cell. 2013; 12:1062–1072. [PubMed: 23834033]
39. Charlton M, Sreekumar R, Rasmussen D, Lindor K, Nair KS. Apolipoprotein synthesis in nonalcoholic steatohepatitis. Hepatology. 2002; 35:898–904. [PubMed: 11915037]
40. Ge X, et al. Aldo-keto reductase 1B7 is a target gene of FXR and regulates lipid and glucose homeostasis. Journal of lipid research. 2011; 52:1561–1568. [PubMed: 21642744]
41. Zhang Y, et al. Activation of the nuclear receptor FXR improves hyperglycemia and hyperlipidemia in diabetic mice. Proceedings of the National Academy of Sciences of the United States of America. 2006; 103:1006–1011. [PubMed: 16410358]
42. Zhang Y, Yin L, Hillgartner FB. SREBP-1 integrates the actions of thyroid hormone, insulin, cAMP, and medium-chain fatty acids on ACCalpha transcription in hepatocytes. Journal of lipid research. 2003; 44:356–368. [PubMed: 12576518]
43. Bligh EG, Dyer WJ. A rapid method of total lipid extraction and purification. Can J Biochem Physiol. 1959; 37:911–917. [PubMed: 13671378]
44. Xu J, et al. Hepatic carboxylesterase 1 is essential for both normal and farnesoid X receptor-controlled lipid homeostasis. Hepatology. 2014; 59:1761–1771. [PubMed: 24038130]
45. Zhang Y, et al. FXR deficiency causes reduced atherosclerosis in Ldlr−/− mice. Arterioscler Thromb Vasc Biol. 2006; 26:2316–2321. [PubMed: 16825595]
46. Zhang Y, et al. Loss of FXR protects against diet-induced obesity and accelerates liver carcinogenesis in ob/ob mice. Mol Endocrinol. 2012; 26:272–280. [PubMed: 22261820]

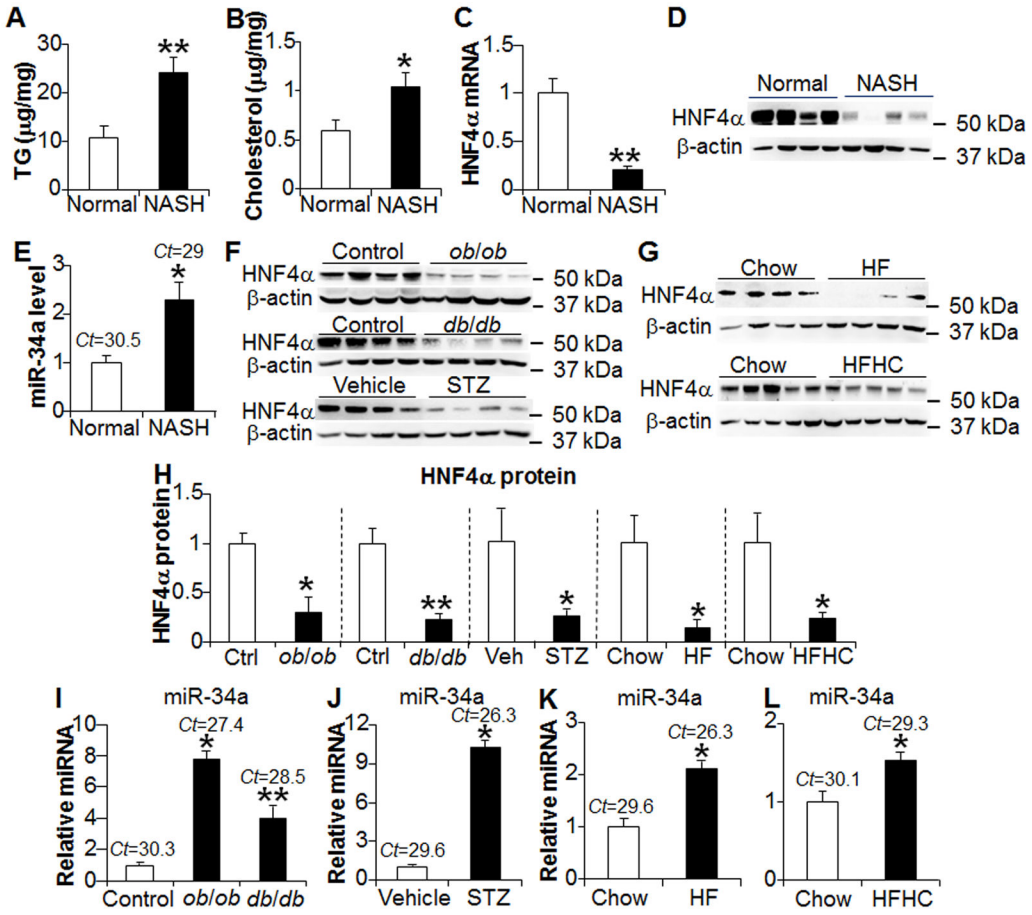

Figure 1. Hepatic HNF4α and miR-34a expression is inversely regulated in NASH patients and diabetic or HFD-fed mice

(**a–e**) Hepatic levels of TG (**a**), cholesterol (**b**), *Hnf4α* mRNA (**c**), HNF4α protein (**d**) and *miR-34a* (**e**) were determined in normal individuals or NASH patients (n=8). (**f–h**) Hepatic HNF4α protein levels were determined using Western blots in diabetic *ob*/*ob* or *db*/*db* mice (**f**; n=5) or STZ-treated mice (**f**; n=6), high fat diet (HFD)-fed mice (**g**; n=5) or high fat, high cholesterol (HFHC) diet-fed mice (**g;** n=8). Protein levels were quantified by ImageJ (**h**). (**i–l**) Hepatic *miR-34a* levels were quantified in *ob*/*ob* or *db*/*db* mice (**i**), STZ-treated mice (**j**), HFD-fed mice (**k**) or HFHC diet-fed mice (**l**). Results are shown as mean±SEM. Two-sided student *t*-test was performed. * $P<0.05$. ** $P<0.01$.

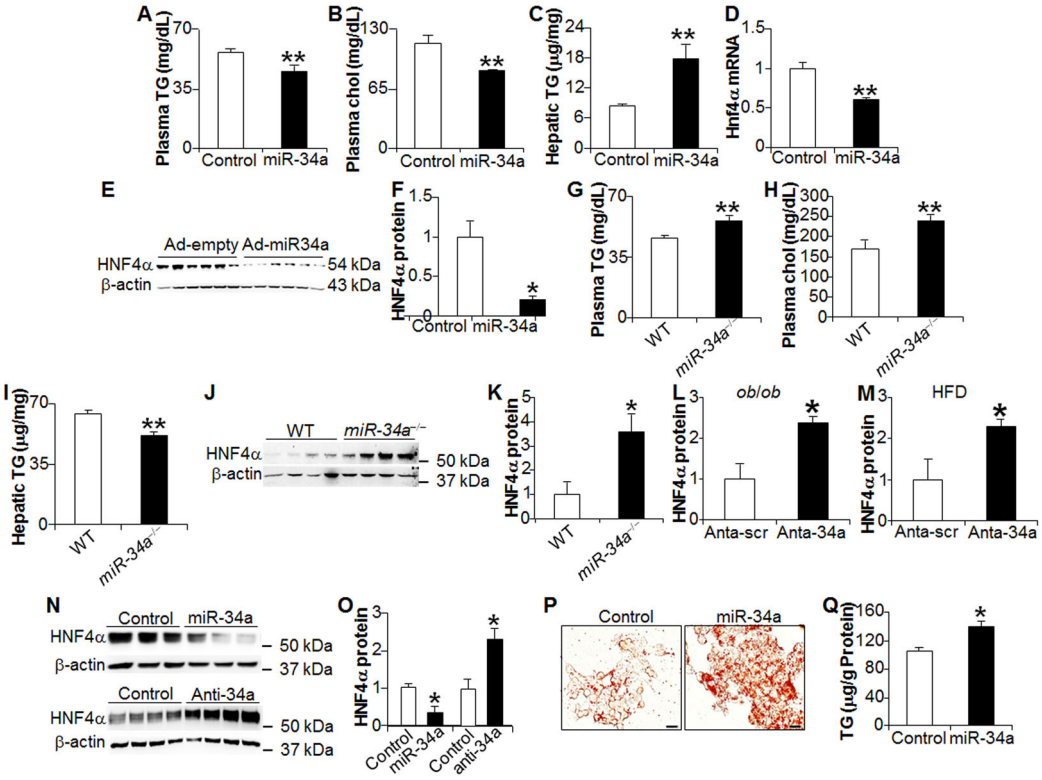

Figure 2. miR-34a regulates lipid metabolism and inhibits HNF4α expression in mice and HepG2 cells

(**a–f**) C57BL/6 mice were injected i.v. with either Ad-empty (control) or Ad-miR-34a (miR-34a) (n=6). After 7 days, plasma TG (**a**), cholesterol (chol; **b**) and hepatic TG (**c**) levels were determined. Hepatic *Hnf4α* mRNA level was quantified by qRT-PCR (**d**). Hepatic protein levels were determined by Western blots (**e**) and then quantified (**f**). (**g–k**) Wild-type and *miR-34a*$^{-/-}$ mice were fed a Western diet for 12 weeks (n=5). Plasma TG (**g**), plasma cholesterol (**h**) and hepatic TG levels (**I**) were determined. Hepatic protein levels were determined by Western blotting (**J**) and HNF4α protein levels quantified (**k**). (**l, m**) *ob*/*ob* mice (**l**) or HFD-fed mice (**m**) were injected i.v. with anta-scr (scramble antagomir) or anta-miR-34a (miR-34a antagomir) once every 6 days (10 mg per kg) (n=4–5). After 3 injections, hepatic HNF4α protein levels were determined. (**n, o**) HepG2 cells were treated with Ad-empty (control), Ad-miR-34a or Ad-anti-miR-34a (anti-miR-34a). After 48 h, protein levels were determined by Western blotting (**n**) and then quantified (**o**) (n=3). (**p, q**) HepG2 cells were infected with Ad-empty or Ad-miR-34a for 48 h. Neutral lipids were stained by oil red O (**p**) and TG levels quantified (**q**) (n=6). The transfection assays were repeated once and similar results were obtained. Scale bar, 20 μm. Values are expressed as mean±SEM. Two-sided student *t*-test was performed. * $P<0.05$, ** $P<0.01$.

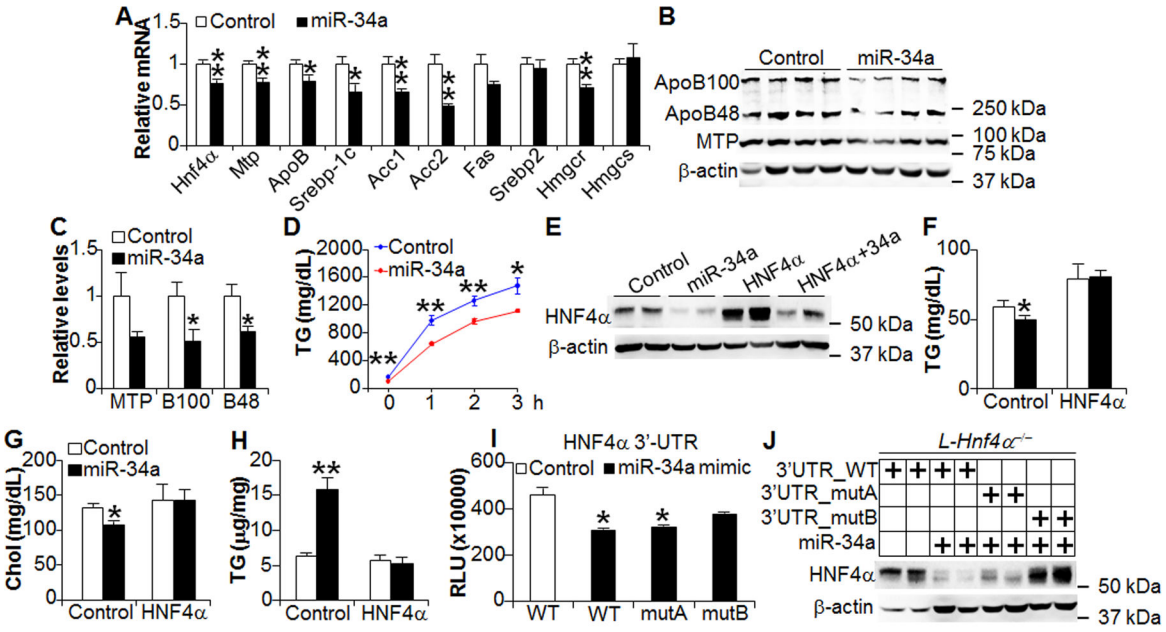

Figure 3. miR-34a regulation of VLDL secretion and lipid metabolism depends on inhibition of hepatic HNF4α

(**a–c**) C57BL/6 mice were i.v. injected with Ad-empty or Ad-miR-34a (n=6). Hepatic mRNA (**a**) and protein levels (**b, c**) were quantified. B100, ApoB100. B48, ApoB48. (**d**) VLDL secretion was determined in C57BL/6 mice after i.p. injection of Tyloxapol (50 mg/kg) (n=6). (**e–h**) C57BL/6 mice were injected i.v. with Ad-empty, Ad-miR-34a, Ad-HNF4α or Ad-miR-34a+Ad-HNF4α (n=7). Hepatic protein levels (**e**), plasma TG (**f**), plasma cholesterol (**g**) and hepatic TG levels (**h**) were determined. (**i**) HepG2 cells were transfected with a control mimic or miR-34a mimic, together with a pMIR-Report construct containing wild-type or mutant 3′ UTR of HNF4α (n=4). After 36 h, luciferase activity was determined and normalized to β-gal activity. MutA and mutB stand for the first or second mutant binding site for miR-34a, respectively. (**j**) Liver-specific *Hnf4α*$^{-/-}$ mice were injected i.v. with Ad-HNF4α-3′UTR (3′UTR_WT), Ad-HNF4α-3′UTR_mutA (3′UTR_mutA) or Ad-HNF4α-3′UTR_mutB (3′UTR_mutB) plus or minus Ad-miR-34a. After 7 days, hepatic protein levels were determined. WT, wild type. Values are expressed as mean±SEM. Two-sided student *t*-test was performed. * $P<0.05$, ** $P<0.01$.

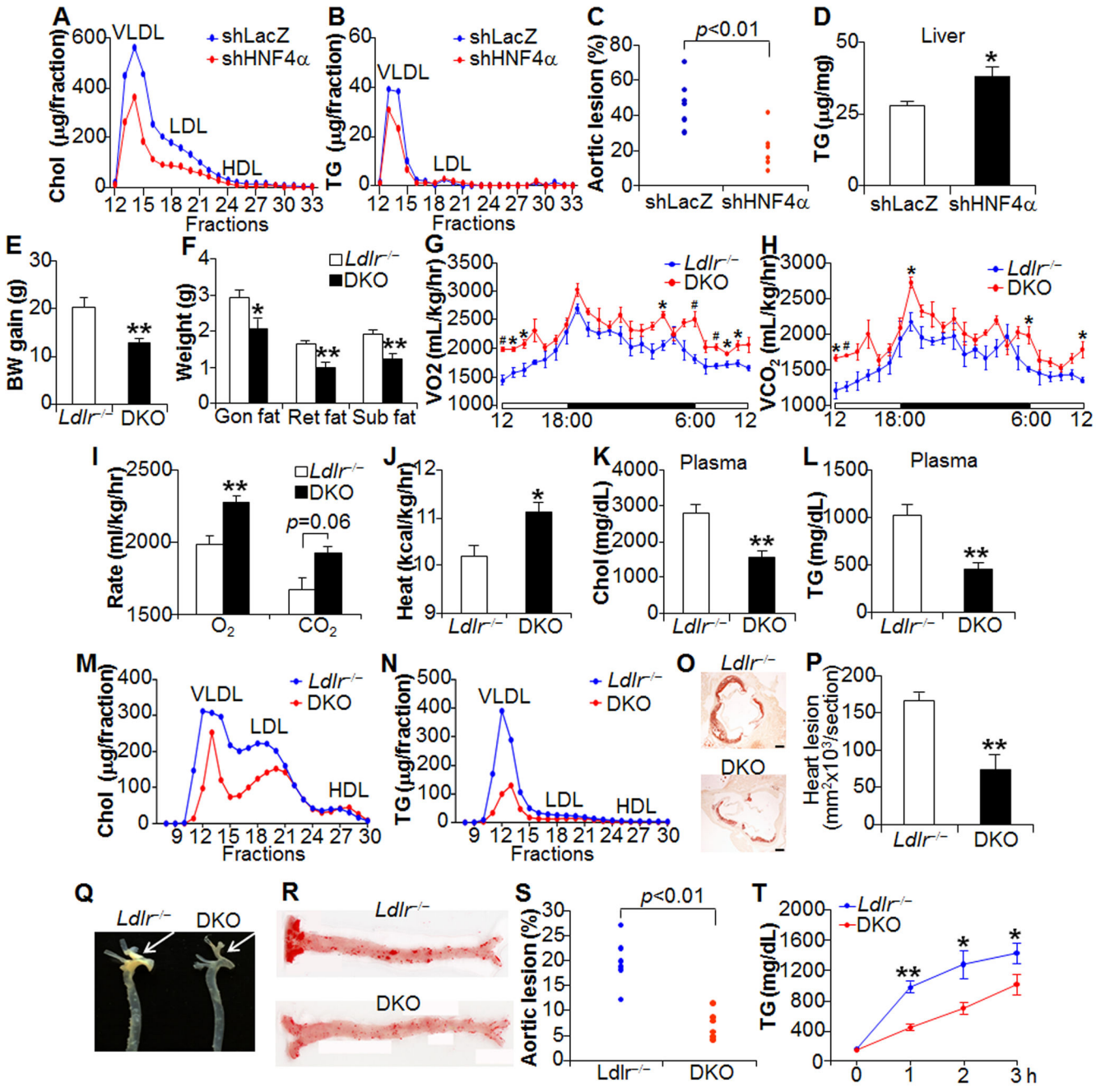

Figure 4. Loss of hepatic HNF4α improves energy homeostasis and protects against atherosclerosis

(**a–d**) *Apoe*$^{-/-}$ mice were fed a Western diet for 4 weeks, followed by injection of Ad-shLacZ or Ad-shHNF4α (n=6). Three weeks following adenoviral injection, plasma cholesterol (**a**) and TG (**b**) lipoprotein profiles were determined. *En face* aortic lesion sizes were analyzed (**c**) and hepatic TG levels quantified (**d**). (**e–t**) *Hnf4α*$^{fl/fl}$*Ldlr*$^{-/-}$ (*Ldlr*$^{-/-}$) mice and *Hnf4α*$^{fl/fl}$*Alb-CreLdlr*$^{-/-}$ (DKO) mice were fed a Western diet for 16 weeks (n=6). Body weight gain (**e**) and body fat content from gonadal (gon) fat, retroperitoneal (ret) fat and subcutaneous (sub) fat (**f**) were determined. O_2 consumption (**g, i**), CO_2 production (**h, i**)

and heat production (**j**) were assessed by CLAMS. Plasma cholesterol (**k**), TG (**l**), cholesterol lipoprotein profile (**m**) and TG lipoprotein profile (**n**) were analyzed. Aortic root was stained by oil red O (**o**) and lesion size quantified (**p**). Aorta was isolated (**q**), stained by oil red O (**r**) and the *en face* lesion size quantified (**s**). VLDL secretion was performed when mice were fed a Western diet for 12 weeks (**t**). In (**Q**), the arrow shows the location of the brachiocephalic artery. Scale bar, 200 μm. Values are expressed as mean±SEM. Two-sided student *t*-test was performed. * $P<0.05$, ** $P<0.01$.

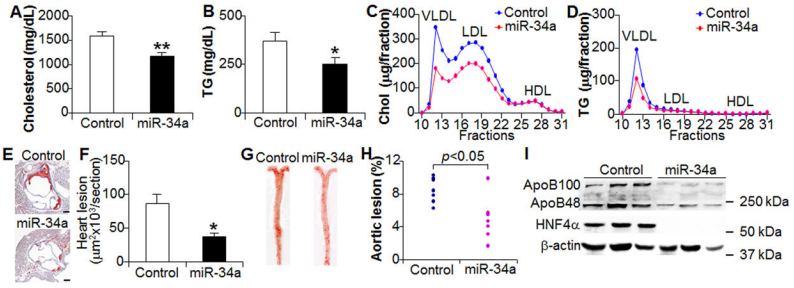

Figure 5. miR-34a reduces the development of atherosclerosis in *Ldlr*$^{-/-}$ mice

Ldlr$^{-/-}$ mice were fed a Western diet for a total of 7 weeks (n=6). At the end of week 4, the mice were injected i.v. with Ad-empty or Ad-miR-34a. Plasma cholesterol (**a**), TG (**b**), cholesterol lipoprotein profile (**c**) and TG lipoprotein profile (**d**) were determined. Aortic root was stained by oil red O (**e**) and lesion size quantified (**f**). Aorta was also stained by oil red O (**g**) and the *en face* lesion size quantified (**h**). Hepatic protein levels were determined by Western blot assays (**i**). Scale bar, 200 μm. Values are expressed as mean±SEM. Two-sided student *t*-test was performed. * $P<0.05$, ** $P<0.01$.

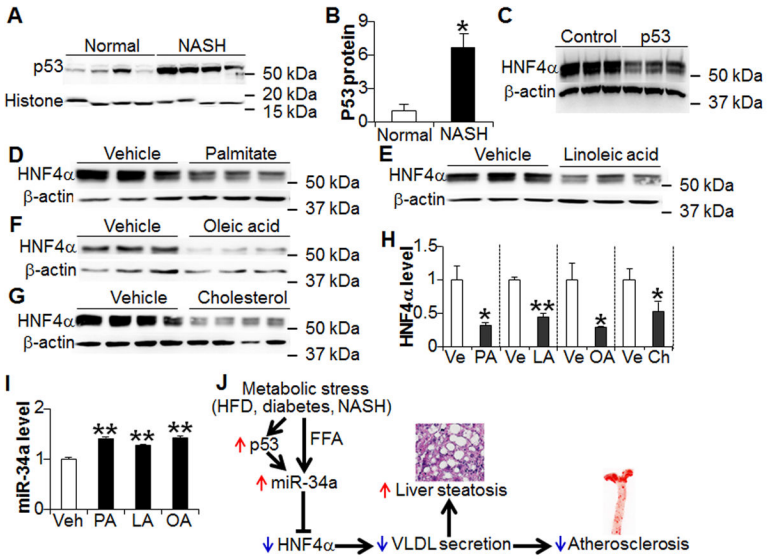

Figure 6. p53, fatty acids and cholesterol regulate the miR-34a-HNF4α pathway

(**a, b**) Nuclear p53 protein levels in the livers of normal individuals and NASH patients were determined by Western blot assays (**a**) and then quantified (**b**). (**c**) HepG2 cells were infected with Ad-empty or Ad-p53. After 48 h, protein levels were determined by Western blot assays. (**d–i**) HepG2 cells were treated with either vehicle (Ve), palmitate (PA; 300 μM) (**d**), linoleic acid (LA; 300 μM) (**e**), oleic acid (OA; 300 μM) (**f**) or cholesterol (Ch;10 μg per ml) (**g**). Western blot assays were performed (**d–g**) and then quantified (**h**). qRT-PCR was used to quantify miR-34a levels (**i**). (**j**) Role of the miR-34a-HNF4α pathway in regulating lipid and lipoprotein metabolism. Under metabolic stress, miR-34a is highly induced via both p53-dependent and -independent pathways. The induction of miR-34a causes a reduction in hepatic HNF4α expression and VLDL secretion, leading to liver steatosis and inhibition of atherogenesis. Values are expressed as mean±SEM. Two-sided student *t*-test was performed. * $P<0.05$, ** $P<0.01$.